

The cosmological impact of future constraints on H_0 from gravitational-wave standard sirens

Eleonora Di Valentino,^{1,*} Daniel E. Holz,^{2,3,†} Alessandro Melchiorri,^{4,‡} and Fabrizio Renzi^{4,§}

¹*Jodrell Bank Center for Astrophysics, School of Physics and Astronomy,
University of Manchester, Oxford Road, Manchester, M13 9PL, UK*

²*Enrico Fermi Institute, Department of Physics, Department of Astronomy and Astrophysics,
and Kavli Institute for Cosmological Physics, University of Chicago, Chicago, IL 60637, USA*

³*Kavli Institute for Particle Astrophysics & Cosmology and Physics Department,
Stanford University, Stanford, CA 94305*

⁴*Physics Department and INFN, Università di Roma “La Sapienza”, Ple Aldo Moro 2, 00185, Rome, Italy*

(Dated: October 2, 2018)

Gravitational-wave standard sirens present a novel approach for the determination of the Hubble constant. After the recent spectacular confirmation of the method thanks to GW170817 and its optical counterpart, additional standard siren measurements from future gravitational-wave sources are expected to constrain the Hubble constant to high accuracy. At the same time, improved constraints are expected from observations of cosmic microwave background (CMB) polarization and from baryon acoustic oscillations (BAO) surveys. We explore the role of future standard siren constraints on H_0 in light of expected CMB+BAO data. Considering a 10-parameters cosmological model, in which curvature, the dark energy equation of state, and the Hubble constant are unbounded by CMB observations, we find that a combination of future CMB+BAO data will constrain the Hubble parameter to $\sim 1.5\%$. Further extending the parameter space to a time-varying dark energy equation of state, we find that future CMB+BAO constraints on H_0 are relaxed to $\sim 3.0\%$. These accuracies are within reach of future standard siren measurements from the Hanford-Livingston-Virgo and the Hanford-Livingston-Virgo-Japan-India networks of interferometers, showing the cosmological relevance of these sources. If future gravitational-wave standard siren measurements reach 1% on H_0 , as expected, they would significantly improve future CMB+BAO constraints on curvature and on the dark energy equation of state by up to a factor ~ 3 . We also show that the inclusion of H_0 constraints from gravitational-wave standard sirens could result in a reduction of the dark energy figure-of-merit (i.e., the cosmological parameter volume) by up to a factor of ~ 400 .

I. INTRODUCTION

Gravitational-wave standard sirens (GWSS) have been proposed as a powerful method for the determination of the Hubble constant (see e.g. [1–9]). The feasibility of the method has been experimentally confirmed by the recent spectacular observations of the event GW170817 [10] and the detection of an associated optical counterpart [11–13], yielding a constraint of $H_0 = 70_{-8}^{+12}$ km/s/Mpc (maximum a posteriori value with minimal 68.3% credible interval) [14]. While this constraint is much weaker than those currently obtained from measurements of luminosity distances of standard sirens or observations of the cosmic microwave background (CMB) anisotropies, it is expected to significantly improve in the coming years with the discovery of additional standard siren events. Moreover, this kind of measurement is clearly of particular interest given the current discrepancy on the value of H_0 between standard candle luminosity distances of Cepheids and Type Ia supernovae, that report a value of $H_0 = 73.24 \pm 1.74$ km/s/Mpc at 68% C.L. [15] (R16,

hereafter), ($H_0 = 73.52 \pm 1.62$ km/s/Mpc at 68% C.L. in the new analysis of [16]), and CMB measurements from the latest Planck satellite 2018 release that gives $H_0 = 67.27 \pm 0.60$ km/s/Mpc at 68% C.L. ([17], see also [18–20]). Current observations of baryon acoustic oscillations (BAO) are in agreement with the Planck cosmology and a combined Planck+BAO analysis gives $H_0 = 67.67 \pm 0.45$ km/s/Mpc at 68% C.L. [17], also in strong discrepancy with the standard candle results of [15, 16].

While unidentified systematics could be clearly present, this tension may indicate the need of new physics beyond the standard Λ CDM model. Indeed, since the Planck constraint is derived under the assumption of Λ CDM, simple extensions to this model could relax the CMB constraint. For example, new physics in the dark energy or neutrino sectors can significantly undermine the Planck constraints on the Hubble constant, solving the current tension on H_0 (see e.g. [15, 21–41]). Moreover, a time varying dark energy equation of state could also alleviate the tension between the Planck+BAO and the R16 constraint (see e.g. [23, 42, 43]). Clearly an independent and accurate future determination of H_0 from GWSS will play a key role in confirming or rejecting the possibility of new physics beyond Λ CDM.

It is to emphasized that an accurate measurement of the Hubble constant, even though it is a low-redshift quantity, can have important consequences for other

* eleonora.divalentino@manchester.ac.uk

† holz@uchicago.edu

‡ alessandro.melchiorri@roma1.infn.it

§ fabrizio.renzi@roma1.infn.it

higher-redshift cosmological parameters such as the dark energy equation of state [44]. The possibility of constraining cosmology with GWSS has been already considered in several previous works (see e.g. [4, 45–54]). Some of these studies analyzed “far future” experiments such as the LISA satellite mission [55] expected to be launched in 2034 or third generation interferometers such as the Einstein Telescope [56] or the Cosmic Explorer [57]. However, recently, in [5] it has been estimated that, depending on the discovery rate of binary neutron stars, a sub-percent determination of the Hubble constant from GWSS could be achieved by the Hanford-Livingston-Virgo (HLV) network as early as during the second year of operation at design sensitivity (~ 2023 [58]). Given the rate uncertainties, a sub-percent measurement may have to wait for two years of the Hanford-Livingston-Virgo-Japan-India (HLVJI) network, which is expected to commence operations $\sim 2024+$. On the other hand, a significant improvement in the observational data is expected from the next CMB and BAO experiments. Future satellite missions such as LiteBIRD [59] and ground based experiments such as CMB-S4 [60] will improve the Planck results thanks to cosmic variance limited measurements of CMB polarization. The LiteBIRD satellite is a JAXA strategic large mission candidate in Phase-A1 (concept development) and is currently scheduled for launch around 2026–2027. A complementary ground-based CMB experiment with the sensitivity of CMB-S4 is at the moment planned after 2023. Similarly, galaxy spectroscopic surveys such as DESI ([61], expected to be completed by 2023) will observe BAO with unprecedented precision.

The level of accuracy on the Hubble constant expected from future CMB+BAO observations can reach the 0.15% level (see e.g. [62]). This could naively appear as an order of magnitude more accurate than future projections for standard sirens constraints. However the CMB+BAO constraint is obtained under the assumption of Λ CDM and, as we show below, can easily be more than one order of magnitude weaker in extended cosmological scenarios. These extended scenarios are of particular interest as they may offer a solution to the existing tension between different measurements of H_0 .

We emphasize that standard sirens constitute a direct measurement of the luminosity distance, obviating the need for a distance ladder. The absolute calibration of the source is provided by the theory of general relativity. The possible systematics associated with standard siren measurements are expected to reside primarily with the instrument, and in particular, with the calibration of the photodetectors which lead directly to the measurement of the amplitude of the gravitational waves [63, 64]. This calibration is expected to be achieved to better than 1% in the near future [65]. Gravitational wave standard siren measurements thus have the potential to provide a particularly clean and robust probe to the sub-percent level. This is to be compared with the case of Type Ia supernovae standard candle measurements, which involve

astronomical calibrators such as Cepheids, and multiple rungs of the distance ladder. It remains unclear whether the supernova systematics can be reduced to the $\sim 1\%$ level (see, e.g., [66, 70, 71]). However, if supernovae achieve this level of accuracy on the measurement of H_0 , then our results apply directly to them as well. Of course, supernovae also offer the opportunity to probe to much higher redshifts than GWSS, and therefore offer additional cosmological constraints.

It is therefore timely to investigate what kind of additional constraints a direct determination of H_0 with $\sim 1\%$ accuracy from GWSS can bring, with the expected completion of new CMB and BAO surveys within the coming decade. In this paper we address this question by forecasting the cosmological constraints from future CMB and BAO surveys in extended cosmological scenarios and by discussing the implications of an additional independent and direct H_0 measurement at the level of 1% from upcoming GWSS sources.

Several previous works have presented forecasts on H_0 from a variety of potential future cosmological datasets. Most notably, Weinberg et al. 2013 [72] performed a thorough analysis of future CMB, BAO, weak lensing, and supernovae data, and presented future constraint on dynamical dark energy and explicitly discussed the impact of a future H_0 prior. In this paper we complement and, in some cases, extend these studies; in detail:

- While most of the previous forecasts have adopted a Fisher Matrix approach, we base our analysis on a Monte Carlo Markov Chain method. This is needed when the posterior distribution of the parameters is strongly non-Gaussian. As we discuss later in this paper this is the case for several key parameters when CMB and CMB+GWSS datasets are considered.
- We use an extended 10-parameter space including not only dynamical dark energy but also possible variations in neutrino masses and in the neutrino effective number. We also discuss the impact of the improvement of the H_0 prior on each of the parameters, as well as on the global Figure of Merit (FoM, hereafter).
- We consider 4 future, post-Planck, CMB experiments (one satellite and three ground-based) discussing the relative advantages and disadvantages of these missions. This is the first time that a similar comparison is presented in these extended parameter space (extended parameter spaces considering the CORE-M5 proposal have been already studied in [62]).
- In addition to the CMB data we conservatively adopt a single additional cosmological probe, namely a BAO dataset from the DESI experiment; we do not incorporate future supernovae or weak lensing measurements. The main goal of this paper

is to demonstrate the kind of improvement a GWSS measurement could bring to a very conservative framework, therefore considering at the same time the largest number of parameters and the smallest number of datasets in order to minimize the presence of theoretical biases and experimental systematics. We choose CMB and BAO data since they should be, in principle, less affected by theoretical and experimental systematics (see e.g. Table I and the discussion in [66]) letting us to produce more accurate forecasts¹. We complement these measurements with the standard siren measurements, which enjoy a similar level of theoretical and experimental purity.

Our paper is structured as follows: in the next section we discuss our methods, in section III we present our results, and in section IV we present our conclusions.

II. METHOD

In this section we describe our forecasting method. We start with a description of the assumed theoretical framework, and then discuss the generation of forecasts for CMB, BAO, and standard sirens constraints.

A. Extended models

As discussed in the introduction, in this paper we consider parameter extensions to the standard Λ CDM model. These models, as we discuss below, are physically plausible, compatible with current observations, and able to solve in some cases the current observed tensions between cosmological datasets. The standard flat Λ CDM model is based on just 6 parameters: the baryon ω_b and cold dark matter ω_c physical energy densities, the amplitude A_S and the spectral index n_S of scalar primordial perturbations, the angular size of the sound horizon at decoupling θ_s and the optical depth at reionization τ . Following [41, 73] we consider variations with the addition of 4 additional parameters:

- Curvature, Ω_k . Most of recent analyses assume a flat universe with $\Omega_k = 0$ since this is considered as

one of the main predictions of inflation. However, inflationary models with non-zero curvature can be conceived (see e.g. [74]). Moreover the recent results from Planck prefer a closed model $\Omega_k > 0$ at more than two standard deviations [20]. Including further data from BAO strongly constrains curvature with $\Omega_k = 0.0002 \pm 0.0021$ at 68% C.L. and perfectly compatible with a flat universe [20]. However this result is obtained in the framework of Λ CDM+ Ω_k , i.e. in one single parameter extension while here we want to analyze a larger parameter space, varying ten parameters at the same time. In this scenario the current Planck+BAO constraints on Ω_k are weaker.

- Neutrino mass, Σm_ν . Neutrino oscillation experiments have demonstrated that neutrinos undergo flavor oscillations and must therefore have small but non-zero masses. However the neutrino absolute mass scale and the mass hierarchy are not yet determined (see e.g. [75] for a recent review). Usually, as in [20], the total neutrino mass scale is fixed to $\Sigma m_\nu = 0.06\text{eV}$, corresponding to the minimal value expected in the normal hierarchy scenario. There is clearly no fundamental reason to limit current analyses to this value and the neutrino mass should be let free to vary.
- Neutrino effective number, N_{eff} . Any particle that decouples from the primordial thermal plasma before the QCD transition could change the number of relativistic particles at recombination increasing N_{eff} from its standard value of 3.046 (see e.g. [76]). An increased value of N_{eff} can help in solving the Hubble constant tension (see e.g. [15]). Reheating at energy scales close to the epoch of neutrino decoupling could on the contrary lower the value of N_{eff} [77].
- Dark energy equation of state w . While current data are in agreement with a cosmological constant, the possibility of having a dark energy equation of state different from -1 is certainly open (see e.g. [22]). Moreover, a time evolution for w helps in solving the coincidence problem of why dark energy and dark matter have similar densities today. In this paper we consider two parametrizations, either w constant with time or the Chevalier-Polarski-Linder parametrization (hereafter CPL) [78, 79]:

$$w(a) = w_0 + (1 - a)w_a \quad (1)$$

where a is the scale factor, w_0 is the equation of state today ($a = 1$) and w_a parametrizes its time evolution. This should be considered as a minimal extension since dark energy time dependences could be more complicated as, for example, in the case of rapid transitions. We consider dark energy perturbations following the approach of [80].

¹ For example, while future weak lensing measurements from large surveys as EUCLID (see e.g. [67]) are extremely promising, systematic errors could limit an accurate determination of the galaxy shapes (see e.g. [68]) and redshifts ([69]). The accurate description of non-linearities and non-Gaussianities in extended scenarios could also become a relevant issue since at the moment most of the current predictions are computed from N-Body simulations that assume Λ CDM. An accurate modeling of all these systematics for a given experimental configuration is currently under study from the weak lensing community and it goes beyond the scope of this work. We therefore do not consider cosmic shear data in our study.

In this paper we consider the following 10 parameters extensions: $\Lambda\text{CDM}+\Omega_k+N_{\text{eff}}+\Sigma m_\nu+w$ and $\Lambda\text{CDM}+\Omega_k+\Sigma m_\nu+w_0+w_a$. While we study extended models, for our simulated data we assume as a fiducial (true) model the standard ΛCDM model with parameters in agreement with the recent Planck constraints [20]: $\omega_b = 0.02225$, $\omega_c = 0.1198$, $\tau = 0.055$, $100\theta_{MC} = 1.04077$, $\Sigma m_\nu = 0.06$ eV and $n_s = 0.9645$. The corresponding derived value of H_0 in this model is $H_0 = 67.3$ km/s/Mpc. The theoretical models and the simulated data are computed with the latest version of the Boltzmann integrator CAMB [81]. Given a simulated dataset and a likelihood that compares data with theory, we extract the constraints on cosmological parameters using the Monte Carlo Markow Chain (MCMC) code COSMO MC² [82].

B. Forecasts for CMB

We produce forecasts on cosmological parameters for future CMB experiments with a well established and common method (see e.g. [62, 83, 84]). Under the assumption of the fiducial model described previously, we compute the theoretical CMB angular spectra for temperature, C_ℓ^{TT} , E and B modes polarization C_ℓ^{EE} and C_ℓ^{BB} , and cross temperature-polarization C_ℓ^{TE} , using the Boltzmann code [81].

Given an experiment with FWHM angular resolution θ and experimental sensitivity w^{-1} (expressed in $[\mu K\text{-arcmin}]^2$), we can introduce an experimental noise for the temperature angular spectra of the form (see e.g. [85]):

$$N_\ell = w^{-1} \exp(\ell(\ell+1)\theta^2/8 \ln 2). \quad (2)$$

A similar expression is used to describe the noise for the polarization spectra with $w_p^{-1} = 2w^{-1}$ (one detector measures two polarization states).

We have then produced synthetic realisations of CMB data assuming different possible future CMB experiments with technical specifications as listed in Table I. In particular, we have considered a possible future CMB satellite experiments such as LiteBIRD [59] and three possible configurations for ground-based telescopes as Stage-III 'wide' (S3wide), Stage-III 'deep' (S3deep) (see [86]), and CMB-S4 (see e.g. [60, 83, 84]).

The simulated experimental spectra are then compared with the theoretical spectra using a likelihood \mathcal{L} given by

$$-2 \ln \mathcal{L} = \sum_l (2l+1) f_{\text{sky}} \left(\frac{D}{|\bar{C}|} + \ln \frac{|\bar{C}|}{|\hat{C}|} - 3 \right), \quad (3)$$

where \hat{C}_l are the theoretical spectra plus noise, while \bar{C}_l are the fiducial spectra plus noise (i.e. our simulated dataset). The quantities $|\bar{C}|$, $|\hat{C}|$ are :

$$|\bar{C}| = \bar{C}_\ell^{TT} \bar{C}_\ell^{EE} \bar{C}_\ell^{BB} - (\bar{C}_\ell^{TE})^2 \bar{C}_\ell^{BB}, \quad (4)$$

$$|\hat{C}| = \hat{C}_\ell^{TT} \hat{C}_\ell^{EE} \hat{C}_\ell^{BB} - (\hat{C}_\ell^{TE})^2 \hat{C}_\ell^{BB}, \quad (5)$$

where D is defined as

$$D = \hat{C}_\ell^{TT} \bar{C}_\ell^{EE} \bar{C}_\ell^{BB} + \bar{C}_\ell^{TT} \hat{C}_\ell^{EE} \bar{C}_\ell^{BB} + \bar{C}_\ell^{TT} \bar{C}_\ell^{EE} \hat{C}_\ell^{BB} - \bar{C}_\ell^{TE} \left(\bar{C}_\ell^{TE} \hat{C}_\ell^{BB} + 2 \hat{C}_\ell^{TE} \bar{C}_\ell^{BB} \right). \quad (6)$$

In what follows we don't consider information from CMB lensing derived from trispectrum data.

C. Forecast for BAO

For the future BAO dataset we consider the DESI experiment [61]. If D_V is the volume averaged distance, this is defined as:

$$D_V(z) \equiv \left[\frac{(1+z)^2 D_A(z)^2 cz}{H(z)} \right]^{\frac{1}{3}} \quad (7)$$

where D_A is the angular diameter distance and $H(z)$ the expansion rate. Under the assumption of the fiducial model described previously, we compute the theoretical values of the ratio r_s/D_V , where r_s is the sound horizon at the drag epoch when photons and baryons decouple, for the different redshifts in the range $z = [0.15 - 1.85]$ listed in Table II. Given the forecast uncertainties reported in [87] for D_A/r_s and $H(z)$, we then compute the uncertainties on r_s/D_V and we show them in Table II. The simulated BAO dataset is finally compared with the theoretical r_s/D_V values through a Gaussian prior.

As a consistency test, we have checked that by using directly the D_A/r_s value and the corresponding uncertainties reported in [87] instead of r_s/D_V , we obtain very similar results with constraints about $\sim 30\%$ weaker on H_0 when combined with CMB-S4 data, in agreement with the results of [88].

In principle it would be possible to forecast BAO data considering D_A/r_s and $H(z)$ as independent measurements. However some small tension (around 1 sigma level) is present between the current constraints from D_A/r_s and $H(z)$ (see e.g. [88], Figure 2 contours in the Top Left and Bottom Left panels for $\Omega_m \sim 0.3$). It is clearly difficult to properly take into account a possible small tension between future D_A/r_s and $H(z)$ measurements that could improve/reduce future BAO constraints. We therefore follow the approach of [86] deriving the expected fractional uncertainties on r_s/D_V for DESI

² <http://cosmologist.info>

Experiment	Beam	Power noise $w^{-1/2}$ [$\mu\text{K-arcmin}$]	ℓ_{max}	ℓ_{min}	f_{sky}
LiteBIRD	30'	4.5	3000	2	0.7
S3deep	1'	4	3000	50	0.06
S3wide	1.4'	8	3000	50	0.4
CMB-S4	3'	1	3000	5, 50	0.4

Table I. Specifications for the different experimental configurations considered in our paper. In case of polarization spectra the noise w^{-1} is multiplied by a factor 2.

Redshift	$\frac{\sigma(r_s/D_V)}{r_s/D_V}$	$\sigma(r_s/D_V)$
0.15	2.57%	0.00595
0.25	1.71%	0.00246
0.35	1.32%	0.00141
0.45	1.08%	0.00093
0.55	0.91%	0.00067
0.65	0.79%	0.00051
0.75	0.70%	0.00040
0.85	0.68%	0.00036
0.95	0.75%	0.00037
1.05	0.77%	0.00036
1.15	0.76%	0.00034
1.25	0.76%	0.00032
1.35	0.83%	0.00033
1.45	0.96%	0.00037
1.55	1.21%	0.00046
1.65	1.89%	0.00069
1.75	2.91%	0.00104
1.85	3.87%	0.00134

Table II. Specifications for the forecast DESI data, obtained by [87].

from the fractional errors on D_A/r_s and $H(z)$ forecasted in [87].

D. Forecast for standard sirens

As stated in the introduction, in this paper we want to address the question of what kind of cosmological information can be obtained from GWSS systems within

the coming decade (i.e. by ~ 2028) when complementary measurements from CMB and BAO surveys will be available. We therefore focus our attention on GW experiments that could be completed in this time-scale: the Hanford-Livingston-Virgo (HLV) network of interferometers during the second year of operation at design sensitivity (~ 2023) and the the Hanford-Livingston-Virgo-Japan-India (HLVJI) network two years after the start of operations (~ 2026) [58]. We do not consider longer-term experiments such as the LISA [55] or DECIGO [89] missions or proposed third generation interferometers such as the Einstein Telescope [56] or the Cosmic Explore [57] that would presumably start operations no sooner than 2030. Moreover, these experiments will be able to determine the luminosity distance of GWSS at higher redshift, opening the possibility to test the acceleration of the universe (i.e. the deceleration parameter), while here we only limit our discussion to the Hubble constant (although black holes standard sirens would probe these high redshifts earlier [90]).

Considering HLV or HLVJI and assuming the optimistic case that all binary neutron star (BNS) systems have detected optical counterparts and associated redshift measurements, the major uncertainty on the projected constraint on H_0 from GWSS comes from the BNS detection rate. The current best estimate of the BNS rate is $R = 1540^{+3200}_{-1220} \text{ Gpc}^{-3}\text{yr}^{-1}$ [91] (median and 90% credible interval) [10]; it is very poorly constrained given that only one BNS event has been detected to date. Following [5] we forecast 4%, 2%, and 1% uncertainties on the measurement of H_0 for the HLV network after two years at design sensitivity (~ 2023) and assuming lower, mean, and upper BNS rates of $R = 320 \text{ Gpc}^{-3}\text{yr}^{-1}$, $R = 1540 \text{ Gpc}^{-3}\text{yr}^{-1}$, and $R = 4740 \text{ Gpc}^{-3}\text{yr}^{-1}$. The corresponding accuracy for the HLVJI network operating after one year of operation (~ 2025) reaches 3%, 1.4%, and 0.8% on H_0 , while after two years it arrives at 2.8%, 1.2%, and 0.7% (see Figure 3 in [5]). By 2028 the HLVJI network would have an additional two years of operation, leading *very roughly* to a factor of $\sqrt{2}$ improvement to 2%, 0.85%, and 0.5%. It is therefore possible that standard siren measurements will reach an accuracy of 1% by 2028 (under the assumption that a majority of BNS mergers have detectable electromagnetic

counterparts). Considering that our fiducial model has $H_0 = 67.3$ km/s/Mpc, we therefore assume a Gaussian prior of $H_0 = 67.3 \pm 0.673$ km/s/Mpc. In what follows we will refer to this (optimistic) prior as GWSS67. On the other hand, we also consider the significantly more pessimistic H_0 prior of 4% ($H_0 = 67.3 \pm 2.7$ km/s/Mpc). This prior, just a factor of ~ 4 smaller than the current GW constraint based on a single event, is clearly extremely conservative but may happen if the BNS rate ends up on the low side (see e.g. [5, 10, 92, 93]). In what follows we will refer to this prior as PGWSS67.

These priors on H_0 are introduced by importance sampling on the models (samples) drawn from our MCMC simulations [82]. In our case this translates into multiplying each sample weight by a Gaussian function, with mean and variance defined by the assumed H_0 prior, evaluated at the value of H_0 in the sample itself. For this to work it is only necessary that the obtained weights are significant for a large fraction of the re-weighted samples; this is a direct consequence of the requirement that the distribution from which the samples are drawn and the importance distribution are not too dissimilar.

III. RESULTS

A. Λ CDM+ Ω_k + Σm_ν + N_{eff} + w Model

We first forecast the constraints on cosmological parameters from future CMB data only, assuming the extended 10 parameter model Λ CDM+ Ω_k + Σm_ν + N_{eff} + w . The constraints on cosmological parameters for the experimental configurations listed in Table I are reported in Table III, while 2D contour plots at 68% C.L. and 95% C.L. between the extra parameters are reported in Figure 1. We find that future experiments, including CMB-S4, will be unable to provide significant additional constraints on geometrical parameters such as H_0 , Ω_k , and w . This is due to the well known geometrical degeneracy that affects CMB observables (see, e.g., [94–96]). CMB-S4 will improve the constraints on n_s , N_{eff} , $\Omega_b h^2$, and $\Omega_c h^2$ by a factor of ~ 2 –5 with respect to LiteBIRD. These parameters are less affected by the geometrical degeneracy, and can thus be better constrained with an improvement in the angular resolution of the experiment. Constraints on neutrino masses will also only see marginal improvement (i.e. $\Sigma m_\nu < 0.32$ eV at 95% C.L. for the strongest case from CMB-S4), which falls short of the sensitivity of $\Delta \Sigma m_\nu \sim 0.05$ eV needed to test the inverted neutrino mass hierarchy at two standard deviations. The neutrino effective number will be, on the contrary, less affected and interesting constraints at the $\Delta N_{\text{eff}} \sim 0.045$ level can be achieved with CMB-S4 even in the case of a very extended parameter space.

It is interesting to investigate how the inclusion of future BAO surveys, such as DESI, can break the geometrical degeneracy and improve the constraints derived from CMB data. Assuming the same Λ CDM fiducial model,

we report the CMB+DESI constraints in Table IV and we show the 2D confidence level contours at 68% C.L. and 95% C.L. in Figure 2. The geometrical parameters are constrained almost equally by all configurations, indicating that the additional constraining power arises from the inclusion of DESI. Curvature is now determined with a 0.1–0.2% accuracy, while the equation of state can be determined with a $\sim 5\%$ accuracy. It is interesting to note that a degeneracy is present between Ω_k , w , and Σm_ν , i.e. the introduction of a neutrino mass limits the CMB+BAO constraints on curvature and w . In addition, after the inclusion of DESI, CMB-S4+DESI provides better constraints by a factor ~ 2 –4 on parameters such as n_s and N_{eff} with respect to LiteBIRD+DESI. The bounds on the sum of neutrino masses are however still affected by the remaining extra parameters (mostly by the anti-correlation with w and the correlation with Ω_k), resulting in a limit of $\Sigma m_\nu < 0.126$ eV at 95% C.L. for the CMB-S4+DESI configuration and $\Sigma m_\nu < 0.202$ eV at 95% C.L. for LiteBIRD+DESI. However the key result for our analysis is the constraint on the Hubble parameter. Again, between the several configurations we consider, CMB-S4+DESI provides the best constraint of $H_0 = 67.4^{+1.0}_{-1.1}$ km/s/Mpc, i.e. an uncertainty on the value of the Hubble constant of the order of $\sim 1.5\%$, while LiteBIRD+DESI gives $H_0 = 67.8^{+1.3}_{-1.5}$ km/s/Mpc with an uncertainty of $\sim 2\%$.

As discussed in the previous section, a similar uncertainty can be reached by the HLVJI network after one year of observations (~ 2025) with a BNS detection rate of $R \geq 1540$ Gpc $^{-3}$ yr $^{-1}$ or by HLV after two years of observations (~ 2023) if the rate is $R \geq 2800$ Gpc $^{-3}$ yr $^{-1}$. For simplicity we have assumed that the standard siren accuracy on H_0 scales as $1/\sqrt{N_{\text{BNS}}}$ where N_{BNS} is the number of observed BNS systems, which is a good approximation for $N \gtrsim 20$ [5]. A first conclusion is that by 2025–2030 standard sirens may offer constraints on H_0 that are comparable in accuracy to those achievable from future CMB+BAO missions at a similar epoch.

Furthermore, given existing estimates of the BNS event rate, an even higher H_0 accuracy may be expected from GWSS. In Table V and in Figure 3 we report the future constraints achievable by a combination of the CMB data and a prior on the Hubble constant with a 1% accuracy (GWSS67). This GWSS67 prior, with respect to the CMB data alone, breaks the geometrical degeneracy and improves significantly the constraints on the corresponding parameters, now producing strong bounds on cosmological parameters such as curvature (0.3% accuracy from CMB-S4+GWSS67) and w (7% accuracy from CMB-S4+GWSS67). The bound on neutrino masses is improved by $\sim 30\%$, while there is no significant improvement on the remaining parameters (N_{eff} , n_s , and the cold dark matter and baryon densities). How would the inclusion of a GWSS measurement of H_0 impact cosmological constraints derived from a CMB+DESI? We answer to this question in Table VI and Figure 4 where we report the constraints achievable from the full combined dataset.

Parameter	LiteBIRD	S3deep	S3wide	CMB-S4
$\Omega_b h^2$	0.02214 ± 0.00023	0.02222 ± 0.00016	$0.02220 \pm 9 \times 10^{-5}$	$0.02219 \pm 5 \times 10^{-5}$
$\Omega_c h^2$	0.1203 ± 0.0042	0.1199 ± 0.0030	0.1198 ± 0.0013	0.1199 ± 0.0010
$100\theta_{\text{MC}}$	1.04075 ± 0.00078	1.04065 ± 0.00033	1.04071 ± 0.00016	1.04071 ± 0.00012
τ	0.054 ± 0.002	0.054 ± 0.010	0.053 ± 0.010	0.055 ± 0.003
H_0	64^{+8}_{-18}	59^{+7}_{-19}	61^{+7}_{-17}	60^{+8}_{-11}
Ω_K	$-0.014^{+0.018}_{-0.005}$	$-0.027^{+0.033}_{-0.010}$	$-0.016^{+0.020}_{-0.006}$	$-0.012^{+0.016}_{-0.004}$
$\log(10^{10} A_s)$	3.092 ± 0.011	3.090 ± 0.021	3.090 ± 0.021	3.093 ± 0.006
n_s	$0.9629^{+0.0073}_{-0.0074}$	0.9656 ± 0.0112	$0.9650^{+0.0048}_{-0.0046}$	0.9648 ± 0.0038
w	$-1.069^{+0.638}_{-0.297}$	$-0.896^{+0.661}_{-0.279}$	$-0.911^{+0.506}_{-0.243}$	$-0.846^{+0.283}_{-0.234}$
N_{eff}	$3.069^{+0.243}_{-0.246}$	3.082 ± 0.141	3.063 ± 0.070	$3.060^{+0.046}_{-0.045}$
Σm_ν	$< 0.594 \text{ eV}$	$< 0.584 \text{ eV}$	$< 0.405 \text{ eV}$	$< 0.322 \text{ eV}$

Table III. Forecasted constraints at 68% C.L. (upper limits at 95% C.L.) from future CMB experiments with specifications listed in Table I in an extended $\Lambda\text{CDM} + \Omega_k + \Sigma m_\nu + N_{\text{eff}} + w$ 10 parameters analysis. A 6 parameters ΛCDM model is assumed as fiducial model. Parameters as H_0 and w are practically unbounded. Ω_k and Σm_ν are also weakly constrained.

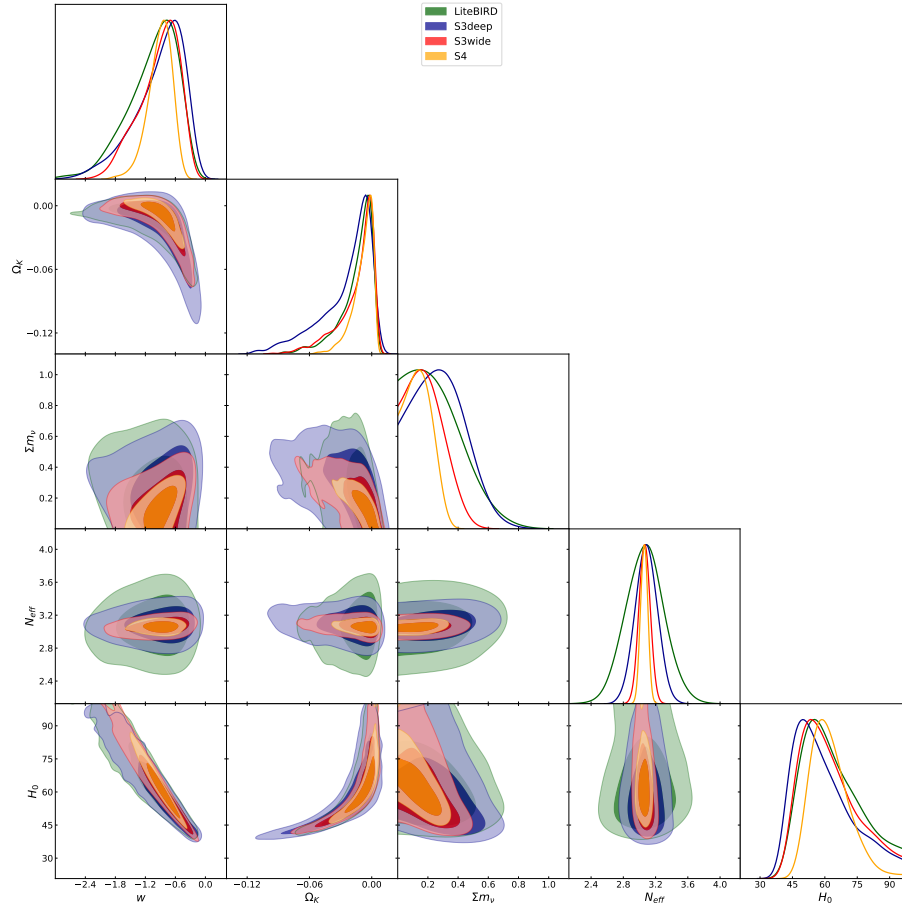


Figure 1. Forecasted future constraints at 68% and 95% C.L. from future CMB data for the experimental configurations in Table I in case of the $\Lambda\text{CDM} + \Omega_k + \Sigma m_\nu + N_{\text{eff}} + w$ extended model. Clearly in this extended parameter space CMB data alone will be unable to significantly constrain geometrical parameters as H_0 , Ω_k or w .

Parameter	LiteBIRD+DESI	S3deep+DESI	S3wide+DESI	CMB-S4+DESI
$\Omega_b h^2$	0.02219 ± 0.00022	0.02219 ± 0.00016	$0.02218 \pm 9 \times 10^{-5}$	$0.02218 \pm 5 \times 10^{-5}$
$\Omega_c h^2$	$0.1212^{+0.0033}_{-0.0041}$	0.1208 ± 0.0027	0.1199 ± 0.0013	0.1199 ± 0.0010
$100\theta_{MC}$	$1.04058^{+0.00071}_{-0.00070}$	1.04069 ± 0.00031	1.04075 ± 0.00015	1.04076 ± 0.00011
τ	0.055 ± 0.002	0.057 ± 0.009	0.057 ± 0.008	$0.055^{+0.002}_{-0.003}$
H_0	$67.8^{+1.3}_{-1.5}$	$67.7^{+1.2}_{-1.3}$	$67.4^{+1.0}_{-1.2}$	$67.4^{+1.0}_{-1.1}$
Ω_K	$0.000^{+0.001}_{-0.002}$	0.001 ± 0.002	0.000 ± 0.001	0.000 ± 0.001
$\log(10^{10} A_s)$	3.097 ± 0.009	3.101 ± 0.018	3.099 ± 0.016	$3.095^{+0.005}_{-0.006}$
n_s	$0.9656^{+0.0069}_{-0.0068}$	0.9637 ± 0.0104	$0.9645^{+0.0046}_{-0.0047}$	$0.9647^{+0.0037}_{-0.0036}$
w	$-1.013^{+0.054}_{-0.047}$	$-1.022^{+0.057}_{-0.047}$	$-1.010^{+0.051}_{-0.045}$	$-1.005^{+0.047}_{-0.043}$
N_{eff}	$3.118^{+0.206}_{-0.237}$	$3.065^{+0.136}_{-0.138}$	3.049 ± 0.067	3.051 ± 0.044
Σm_ν	$< 0.202 \text{ eV}$	$< 0.253 \text{ eV}$	$< 0.186 \text{ eV}$	$< 0.126 \text{ eV}$

Table IV. Forecasted constraints at 68% C.L. (upper limits at 95% C.L.) from future CMB experiments with specifications listed in Table I plus information from the BAO DESI galaxy survey in an extended $\Lambda\text{CDM} + \Omega_k + \Sigma m_\nu + N_{\text{eff}} + w$, 10 parameters, analysis. A 6 parameters ΛCDM model is assumed as fiducial model. When comparing the results with those in the CMB alone case reported in Table III we can notice a significant improvement in geometrical parameters as H_0 , w and Ω_k . Constraints on neutrino masses are also improved.

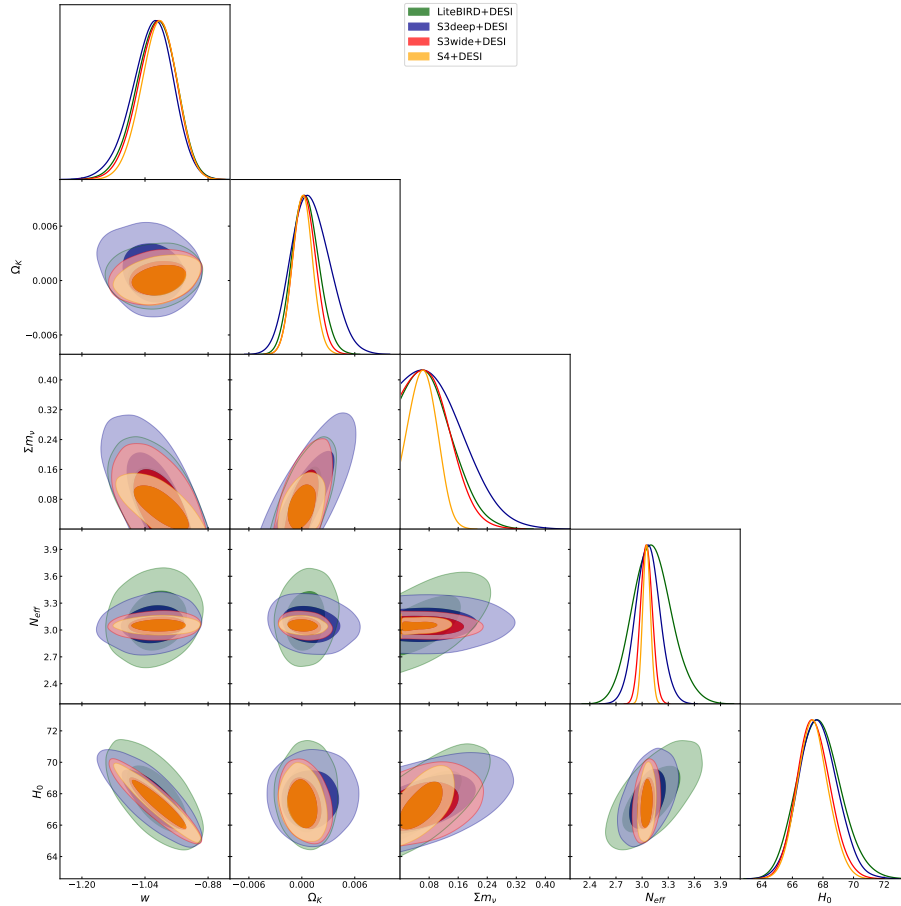


Figure 2. Forecasted constraints at 68% and 95% C.L. from CMB+DESI data for the experimental configurations in Table I in case of the $\Lambda\text{CDM} + \Omega_k + \Sigma m_\nu + N_{\text{eff}} + w$ extended model.

Parameter	LiteBIRD+GWSS67	S3deep+GWSS67	S3wide+GWSS67	CMB-S4+GWSS67
$\Omega_b h^2$	0.02215 ± 0.00023	0.02221 ± 0.00017	$0.02220 \pm 9 \times 10^{-5}$	$0.02219 \pm 5 \times 10^{-5}$
$\Omega_c h^2$	$0.1204^{+0.0042}_{-0.0043}$	$0.1199^{+0.0032}_{-0.0030}$	$0.1198^{+0.0014}_{-0.0013}$	$0.1200^{+0.0010}_{-0.0009}$
$100\theta_{MC}$	1.04075 ± 0.00080	$1.04068^{+0.00031}_{-0.00035}$	$1.04074^{+0.00015}_{-0.00016}$	1.04075 ± 0.00011
τ	0.055 ± 0.002	0.054 ± 0.010	0.053 ± 0.011	$0.055^{+0.002}_{-0.003}$
H_0	$67.30^{+0.67}_{-0.68}$	$67.30^{+0.65}_{-0.67}$	$67.26^{+0.66}_{-0.63}$	67.27 ± 0.65
Ω_K	$-0.005^{+0.007}_{-0.005}$	$-0.006^{+0.007}_{-0.008}$	-0.004 ± 0.005	-0.001 ± 0.003
$\log(10^{10} A_s)$	3.093 ± 0.010	$3.091^{+0.022}_{-0.023}$	3.090 ± 0.022	$3.095^{+0.005}_{-0.006}$
n_s	$0.9631^{+0.0072}_{-0.0074}$	$0.9658^{+0.0117}_{-0.0104}$	$0.9653^{+0.0049}_{-0.0047}$	$0.9649^{+0.0035}_{-0.0037}$
w	$-1.199^{+0.260}_{-0.112}$	$-1.208^{+0.241}_{-0.142}$	$-1.100^{+0.126}_{-0.086}$	$-1.032^{+0.070}_{-0.046}$
N_{eff}	$3.073^{+0.243}_{-0.255}$	$3.076^{+0.147}_{-0.141}$	3.059 ± 0.070	$3.055^{+0.044}_{-0.043}$
Σm_ν	$< 0.587 \text{ eV}$	$< 0.536 \text{ eV}$	$< 0.326 \text{ eV}$	$< 0.206 \text{ eV}$

Table V. Forecasted constraints at 68% C.L. (upper limits at 95% C.L.) from CMB+GWSS67 data for the experimental configurations in Table I in case of the Λ CDM+ Ω_k + Σm_ν + N_{eff} + w extended model.

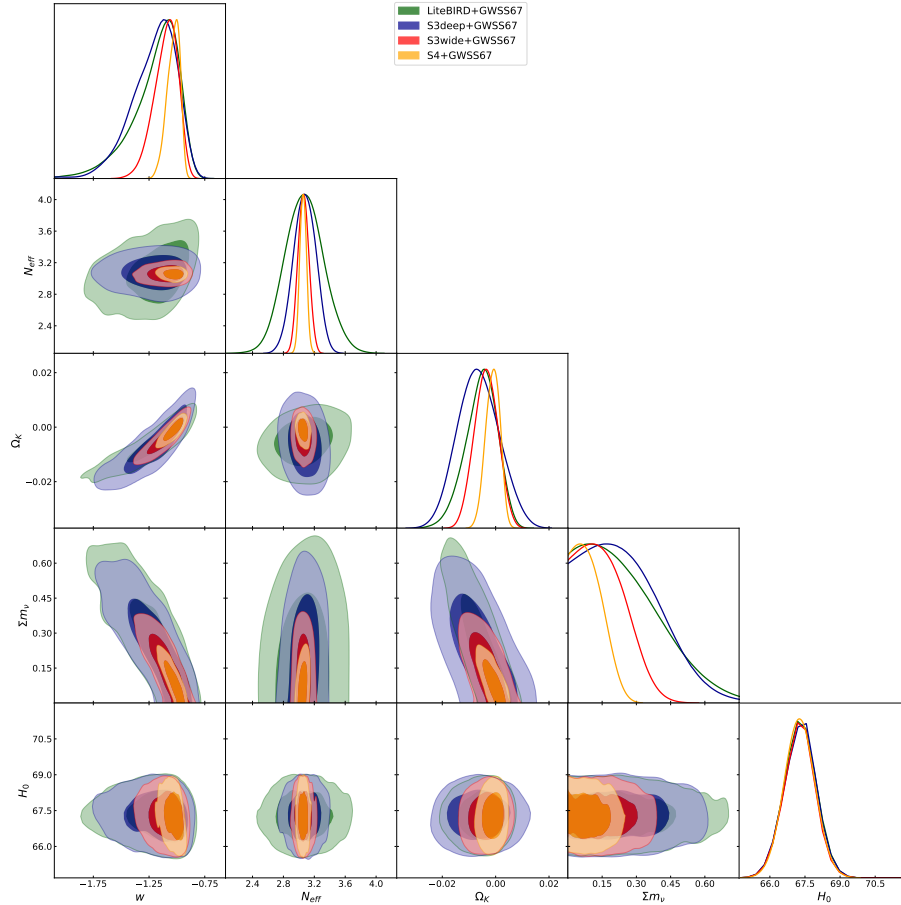


Figure 3. Forecasted constraints at 68% and 95% C.L. from CMB+GWSS67 data for the experimental configurations in Table I in case of the Λ CDM+ Ω_k + Σm_ν + N_{eff} + w extended model.

We find that the combined analysis (in the case of CMB-S4) would constrain the Hubble constant with an accuracy of ~ 0.5 km/s/Mpc, i.e. nearly a factor of two better than the CMB-S4+DESI case. A similar improvement is present with respect to LiteBIRD+DESI. Constraints on the dark energy equation of state are also significantly improved, by 30–40%, reaching an accuracy of about 3% with CMB-S4+DESI and 4% with LiteBIRD+DESI.

It is interesting to note that the constraints on H_0 , Ω_k , and w coming from a combined analysis of DESI, GWSS, and a CMB mission such as LiteBIRD, S3deep, or S3wide, will be comparable or in some cases even better than the corresponding constraints coming from a CMB-S4+DESI dataset. For example, a 0.1% accuracy on curvature or a 3% accuracy on w can be reached by a S3wide+DESI+GWSS67 configuration instead of CMB-S4+DESI. Alternatively, the GWSS measurement would also provide an interesting consistency check between different CMB+BAO datasets.

We also consider the possibility that future standard siren measurements of H_0 will confirm the current tension on the Hubble constant between CMB+BAO and local measurements from supernovae. It is interesting to evaluate at how many standard deviations a CMB+DESI measurement of H_0 will disagree with a GWSS determination of $H_0 = 73.30 \pm 0.73$ km/s/Mpc. From Table IV, we find that the standard siren measurement would be 4 standard deviations from the expected LiteBIRD+DESI constraint, and at roughly 5 standard deviations from the CMB-S4+DESI value. This is a significant improvement, since in an extended parameter space such the one we are considering the existing tension is at about 2 standard deviations (see e.g. [21]).

Finally, let us consider a significantly more pessimistic GW prior on H_0 with a $\sim 4\%$ accuracy (PGWSS67). In Table VII we report the constraints achievable from a combination of this prior with future CMB data. As expected, the constraints on curvature and w are relaxed respect to the previous analyses of CMB+GWSS67 but only by a $\sim 10 - 20\%$. In practice, the geometrical degeneracies between cosmological parameters present in CMB data only can be already sufficiently broken with a, pessimistic, PGWSS67 prior. An improvement of a factor four in the determination of H_0 will result in a, more modest, 10% improvement in the parameters. A first conclusion is therefore that in this theoretical framework, the GWSS67 and the PGWSS67 prior produce very similar constraints when combined with CMB data. On the other hand, combining the PGWSS67 prior with CMB+DESI data has a small effect in improving the constraints on w . We have found that in this case the constraints on w improve just by $\sim 5\%$ while, as discussed above, the improvement in case of GWSS67 is larger than $\sim 20\%$. The 4% PGWSS67 prior will clearly provide little help in solving the current tension on the value of the Hubble parameter.

B. Λ CDM+ Ω_k + Σm_ν + w_a + w_0 Model

As shown in the previous section, the neutrino effective number N_{eff} will be measured with good accuracy even in extended parameter spaces. The main reason for this is due to the lack of the so-called early integrated Sachs Wolfe effect in polarization data. The inclusion of polarization helps in determining the amplitude of the EISW and N_{eff} .

Since we are interested in evaluating the impact of a future GWSS measurement of H_0 , it makes sense to further extend the number of geometric parameters. In what follows we substitute N_{eff} with w_a , considering therefore a dynamical dark energy equation of state described by a CPL form.

In Table VIII we report the constraints at 68% C.L. on cosmological parameters from the combination of future CMB and DESI data while in Figure 5 we report the corresponding 2D contours for the 68% and 95% confidence levels. If we compare with the results in Table VIII and in Figure 5 with those previously obtained assuming $w = \text{constant}$ in Table IV and in Figure 2 there is now a substantial increase (about a factor two!) in the error on H_0 . Indeed, now the combination of CMB-S4+DESI data is able to constrain the Hubble constant to only ~ 2 km/s/Mpc error, i.e. to a $\sim 3\%$ accuracy. LiteBIRD+DESI constrains H_0 to $\sim 3.5\%$ accuracy. These weaker constraints are due to the geometrical degeneracy between H_0 , w_a , and w_0 . The two dark energy parameters are now weakly determined, with uncertainties of the order of $\sim 20\%$ for w_0 and $\sim 60-70\%$ for w_a . H_0 , w_a , and w_0 are also determined to similar accuracy by different CMB experiments, indicating that the constraining power in this case is coming primarily from DESI. The constraint on Ω_k is virtually unchanged with respect to Table IV, and varies with the CMB experiment considered. The inclusion of w_a weakens the future constraint on the sum of neutrino masses, Σm_ν . Other parameters, such as n_s , that are degenerate with N_{eff} , are, on the contrary, now better constrained.

Given the strong degeneracy in the w_0 - w_a plane for these future experiments, it is clearly interesting to study the impact of a future GWSS determination of H_0 . As discussed in the previous section, a 3% accuracy on H_0 can be reached by the HLV network after two years of operation if the BNS detection rate is $R > 3500$ Gpc $^{-3}$ yr $^{-1}$, a value well inside current limits. The same accuracy can be achieved by the HLVJI network after just one year of observation even assuming the lowest BNS rate of $R = 320$ Gpc $^{-3}$ yr $^{-1}$. We found that including a 3% GWSS prior to the CMB+DESI constraints reported in Table VIII the constraints on H_0 and on the dark energy parameters could be already improved at the level of 10 – 30%.

However, a $\sim 1\%$ accuracy on H_0 is also directly attainable by future GWSS measurements, and it is interesting to discuss the impact of this improved determination on future combined cosmological parameter mea-

Parameter	LiteBIRD+DESI+GWSS67	S3deep+DESI+GWSS67	S3wide+DESI+GWSS67	CMB-S4+DESI+GWSS67
$\Omega_b h^2$	0.02218 ± 0.00021	$0.02218^{+0.00015}_{-0.00016}$	$0.02218 \pm 9 \times 10^{-5}$	$0.02218 \pm 5 \times 10^{-5}$
$\Omega_c h^2$	$0.1205^{+0.0028}_{-0.0031}$	0.1205 ± 0.0024	0.1199 ± 0.0013	0.1199 ± 0.0010
$100\theta_{MC}$	$1.04069^{+0.00064}_{-0.00063}$	1.04072 ± 0.00030	1.04075 ± 0.00015	1.04076 ± 0.00011
τ	0.055 ± 0.002	0.057 ± 0.009	0.057 ± 0.008	$0.055^{+0.002}_{-0.003}$
H_0	$67.37^{+0.60}_{-0.61}$	$67.36^{+0.58}_{-0.59}$	67.32 ± 0.57	$67.31^{+0.54}_{-0.55}$
Ω_K	$0.000^{+0.001}_{-0.002}$	0.001 ± 0.002	0.000 ± 0.001	0.000 ± 0.001
$\log(10^{10} A_s)$	3.096 ± 0.008	3.100 ± 0.018	3.099 ± 0.016	$3.095^{+0.005}_{-0.006}$
n_s	0.9648 ± 0.0061	0.9635 ± 0.0100	0.9645 ± 0.0046	0.9648 ± 0.0036
w	$-1.003^{+0.043}_{-0.039}$	$-1.009^{+0.038}_{-0.035}$	-1.007 ± 0.030	-1.003 ± 0.028
N_{eff}	$3.076^{+0.176}_{-0.178}$	$3.053^{+0.124}_{-0.123}$	$3.048^{+0.065}_{-0.066}$	$3.052^{+0.043}_{-0.044}$
Σm_ν	$< 0.164 \text{ eV}$	$< 0.226 \text{ eV}$	$< 0.180 \text{ eV}$	$< 0.120 \text{ eV}$

Table VI. Forecasted constraints at 68% C.L. (upper limits at 95% C.L.) from CMB+DESI+GWSS67 data for the experimental configurations in Table I in case of the Λ CDM+ Ω_k + Σm_ν + N_{eff} + w extended model.

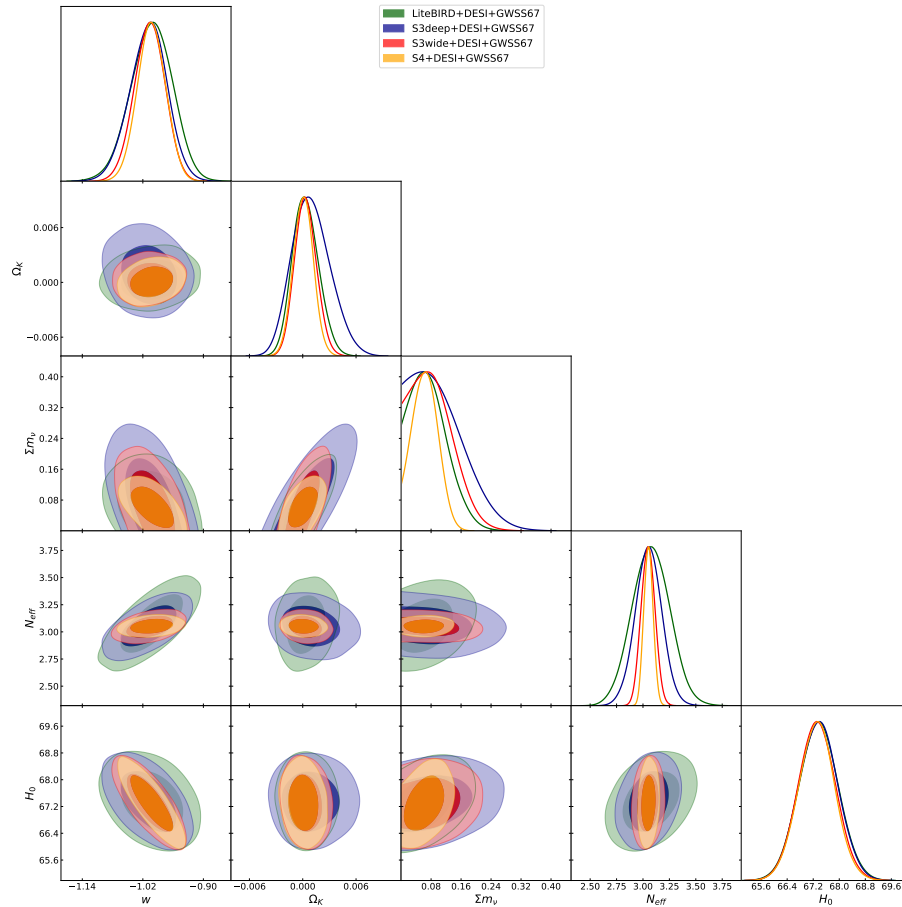


Figure 4. Forecasted constraints at 68% and 95% C.L. from CMB+DESI+GWSS67 data for the experimental configurations in Table I in case of the Λ CDM+ Ω_k + Σm_ν + N_{eff} + w extended model.

Parameter	LiteBIRD+PGWSS67(4%)	S3deep+PGWSS67(4%)	S3wide+PGWSS67(4%)	S4+PGWSS67(4%)
$\Omega_b h^2$	0.02215 ± 0.00023	0.02222 ± 0.00017	$0.02219 \pm 9 \times 10^{-5}$	$0.02219 \pm 5 \times 10^{-5}$
$\Omega_c h^2$	$0.1204^{+0.0040}_{-0.0044}$	$0.1199^{+0.0031}_{-0.0029}$	$0.1198^{+0.0014}_{-0.0013}$	$0.1200^{+0.0010}_{-0.0011}$
$100\theta_{\text{MC}}$	$1.04073^{+0.00079}_{-0.00078}$	$1.04068^{+0.00034}_{-0.00033}$	1.04074 ± 0.00015	1.04075 ± 0.00012
τ	0.055 ± 0.002	0.054 ± 0.010	0.053 ± 0.011	$0.055^{+0.002}_{-0.003}$
H_0	67.03 ± 2.68	$66.95^{+2.65}_{-2.69}$	$66.86^{+2.80}_{-2.69}$	$66.72^{+2.52}_{-2.55}$
Ω_K	$-0.006^{+0.007}_{-0.005}$	-0.007 ± 0.008	$-0.004^{+0.005}_{-0.004}$	-0.002 ± 0.003
$\log(10^{10} A_s)$	3.093 ± 0.010	3.090 ± 0.022	3.090 ± 0.021	$3.094^{+0.005}_{-0.006}$
n_s	$0.9631^{+0.0073}_{-0.0074}$	$0.9662^{+0.0109}_{-0.0111}$	$0.9651^{+0.0046}_{-0.0049}$	$0.9652^{+0.0040}_{-0.0039}$
w_0	$-1.188^{+0.274}_{-0.130}$	$-1.191^{+0.254}_{-0.151}$	$-1.087^{+0.148}_{-0.112}$	$-1.022^{+0.088}_{-0.079}$
N_{eff}	$3.073^{+0.244}_{-0.247}$	$3.078^{+0.142}_{-0.140}$	$3.056^{+0.068}_{-0.069}$	$3.058^{+0.047}_{-0.048}$
m_ν	$< 0.580 \text{ eV}$	$< 0.531 \text{ eV}$	$< 0.338 \text{ eV}$	$< 0.208 \text{ eV}$

Table VII. Forecasted constraints at 68% C.L. (upper limits at 95% C.L.) from CMB+PGWSS67 data for the experimental configurations in Table I in case of the $\Lambda\text{CDM}+\Omega_k+\Sigma m_\nu+N_{\text{eff}}+w$ extended model.

Parameter	LiteBIRD+DESI	S3wide+DESI	S3deep+DESI	CMB-S4+DESI
$\Omega_b h^2$	0.02214 ± 0.00018	$0.02218 \pm 6 \times 10^{-5}$	0.02217 ± 0.00011	$0.02218 \pm 3 \times 10^{-5}$
$\Omega_c h^2$	0.1201 ± 0.0011	0.1199 ± 0.0009	$0.1207^{+0.0018}_{-0.0020}$	0.1198 ± 0.0008
$100\theta_{\text{MC}}$	1.04072 ± 0.00049	1.04075 ± 0.00013	1.04070 ± 0.00028	1.04077 ± 0.00010
τ	0.055 ± 0.002	0.057 ± 0.009	0.057 ± 0.009	$0.055^{+0.002}_{-0.003}$
H_0	66.2 ± 2.3	66.3 ± 2.3	66.4 ± 2.4	$66.4^{+2.2}_{-1.9}$
Ω_K	0.000 ± 0.002	0.000 ± 0.002	0.001 ± 0.003	0.000 ± 0.001
$\log(10^{10} A_s)$	3.095 ± 0.004	3.098 ± 0.017	3.100 ± 0.018	3.094 ± 0.005
n_s	0.9638 ± 0.0042	0.9644 ± 0.0026	$0.9626^{+0.0060}_{-0.0059}$	0.9645 ± 0.0023
w_0	$-0.859^{+0.202}_{-0.259}$	$-0.883^{+0.203}_{-0.252}$	$-0.872^{+0.225}_{-0.269}$	$-0.901^{+0.149}_{-0.228}$
w_a	$-0.470^{+0.795}_{-0.540}$	$-0.390^{+0.749}_{-0.549}$	$-0.456^{+0.818}_{-0.616}$	$-0.306^{+0.661}_{-0.372}$
Σm_ν	$< 0.212 \text{ eV}$	$< 0.216 \text{ eV}$	$< 0.289 \text{ eV}$	$< 0.150 \text{ eV}$

Table VIII. Forecasted constraints at 68% C.L. (upper limits at 95% C.L.) from CMB+DESI data for the experimental configurations in Table I in case of the $\Lambda\text{CDM}+\Omega_k+\Sigma m_\nu+w+w_a$ extended model. Note the significant increase in the error on H_0 (about a factor two) with respect to the $\Lambda\text{CDM}+\Omega_k+\Sigma m_\nu+N_{\text{eff}}+w$ scenario reported before.

measurements. We report the constraints on cosmological parameters for CMB+DESI+GWSS67 in Table IX and the corresponding 2D confidence levels in Figure 6. The measured value of the Hubble constant is practically identical to the assumed prior from the standard sirens (GWSS67), indicating that the standard siren measurements are contributing to the combined constraints on all related cosmological parameters. In particular, the constraints on the dark energy parameters w_0 and w_a are substantially improved, by a factor ~ 1.6 – 2.8 , with the inclusion of the standard siren measurements.

Finally, in Table X we report the expected constraints when combining future CMB data with a, pessimistic, PGWSS67 prior on the Hubble parameter. As we can see, including the PGWSS67 prior will improve the constraints on the dark energy parameters by ~ 20 – 30% respect to CMB+DESI data. A $\sim 4\%$ determination of the Hubble parameter can be therefore useful in this theoretical framework even when considering the CMB+DESI dataset. However the constraints achievable with the PGWSS67 prior on w_0 will be about a factor two larger than those achievable with the GWSS67 prior.

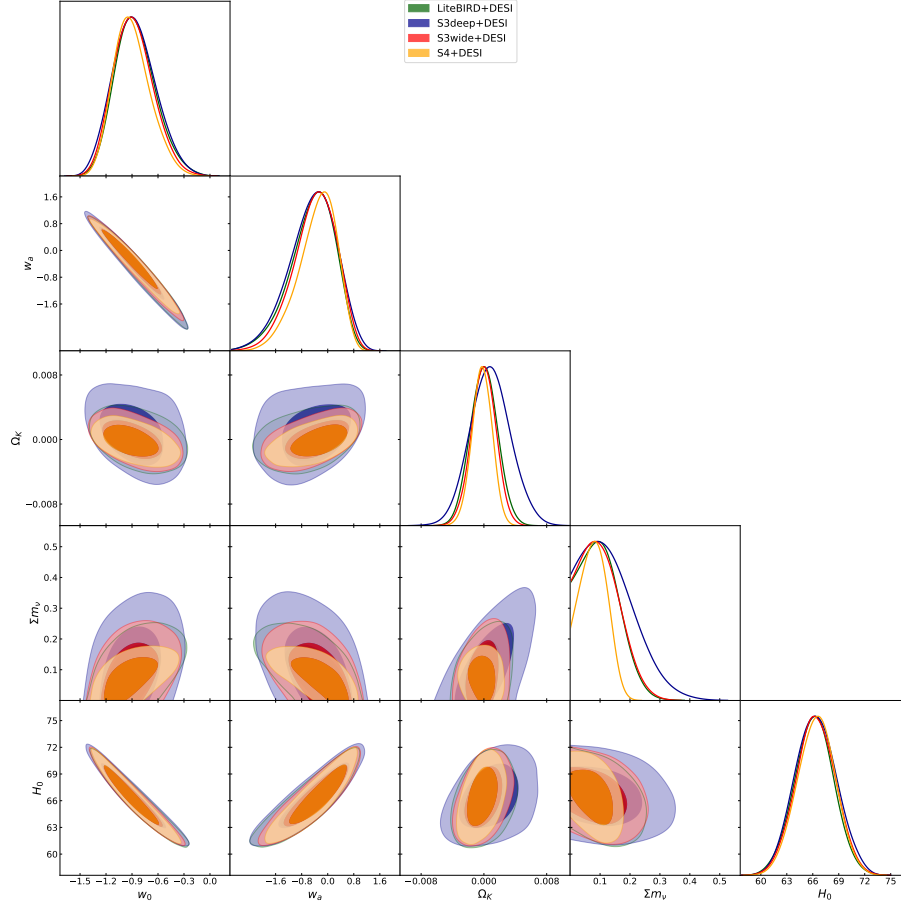


Figure 5. Forecasted constraints at 68% and 95% C.L. from CMB+DESI data for the experimental configurations in Table I in case of the Λ CDM+ Ω_k + Σm_ν + w_0 + w_a extended model.

Parameter	LiteBIRD+DESI+GWSS67	S3wide+DESI+GWSS67	S3deep+DESI+GWSS67	CMB-S4+DESI+GWSS67
$\Omega_b h^2$	0.02214 ± 0.00017	$0.02218 \pm 5 \times 10^{-5}$	0.02217 ± 0.00012	$0.02218 \pm 3 \times 10^{-5}$
$\Omega_c h^2$	$0.1202^{+0.0010}_{-0.0011}$	0.1200 ± 0.0009	$0.1207^{+0.0017}_{-0.0020}$	0.1198 ± 0.0008
$100\theta_{\text{MC}}$	1.04074 ± 0.00048	1.04075 ± 0.00013	1.04070 ± 0.00028	1.04077 ± 0.00010
τ	0.055 ± 0.002	0.057 ± 0.008	0.057 ± 0.009	0.055 ± 0.002
H_0	$67.21^{+0.62}_{-0.63}$	$67.23^{+0.67}_{-0.63}$	67.24 ± 0.64	$67.23^{+0.63}_{-0.64}$
Ω_K	0.000 ± 0.002	0.000 ± 0.001	0.001 ± 0.002	0.000 ± 0.001
$\log(10^{10} A_s)$	3.095 ± 0.004	$3.098^{+0.016}_{-0.017}$	3.100 ± 0.018	3.095 ± 0.005
n_s	0.9638 ± 0.0043	0.9642 ± 0.0026	0.9625 ± 0.0058	0.9644 ± 0.0022
w_0	$-0.974^{+0.078}_{-0.089}$	$-0.978^{+0.081}_{-0.089}$	$-0.969^{+0.084}_{-0.095}$	$-0.985^{+0.066}_{-0.082}$
w_a	$-0.147^{+0.377}_{-0.282}$	$-0.127^{+0.360}_{-0.304}$	$-0.188^{+0.404}_{-0.320}$	$-0.080^{+0.319}_{-0.225}$
Σm_ν	$< 0.196 \text{ eV}$	$< 0.205 \text{ eV}$	$< 0.278 \text{ eV}$	$< 0.140 \text{ eV}$

Table IX. Forecasted constraints at 68% C.L. (upper limits at 95% C.L.) from CMB+DESI+GWSS67 data for the experimental configurations in Table I in case of the Λ CDM+ Ω_k + Σm_ν + w + w_a extended model. Note the significant improvement in accuracy on H_0 and on the dark energy parameters w_0 and w_a with respect to the CMB+DESI case.

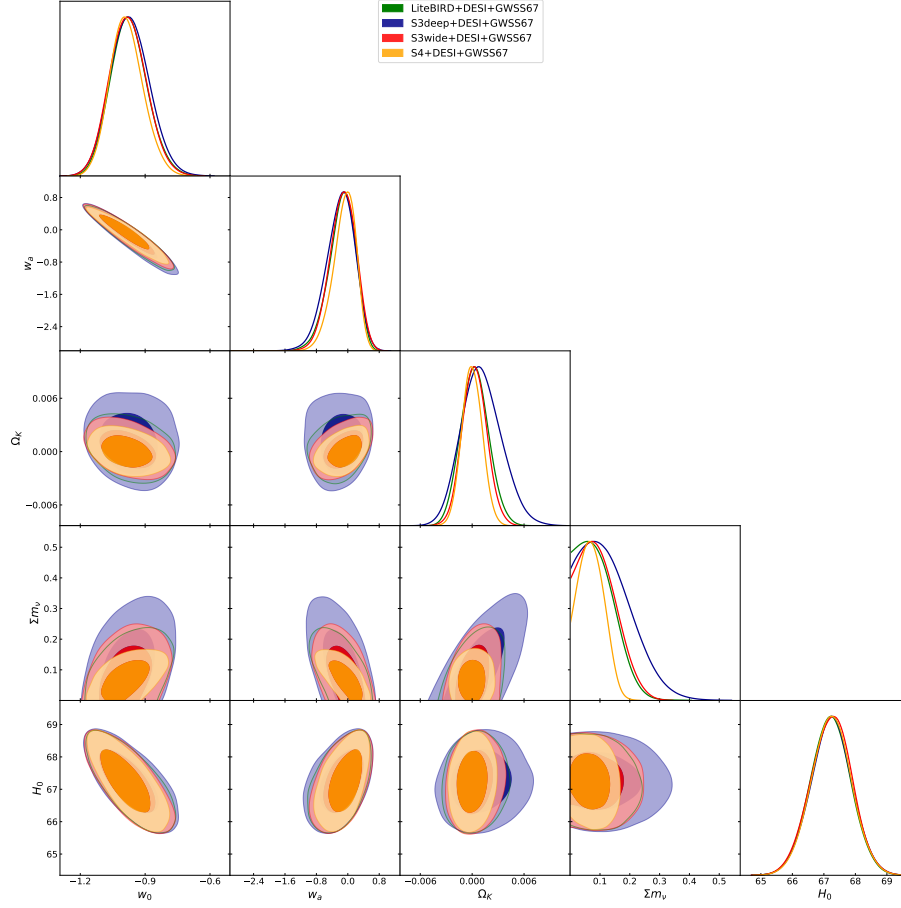


Figure 6. Forecasted constraints at 68% and 95% C.L. from CMB+DESI+GWSS67 data for the experimental configurations in Table I in case of the Λ CDM+ Ω_k + Σm_ν + w_0 + w_a extended model.

Parameter	LiteBIRD+DESI+PGWSS67	S3wide+DESI+PGWSS67	S3deep+DESI+PGWSS67	CMB-S4+DESI+PGWSS67
$\Omega_b h^2$	0.02214 ± 0.00017	0.02217 ± 0.00011	$0.02218 \pm 6 \times 10^{-5}$	$0.02218 \pm 3 \times 10^{-5}$
$\Omega_c h^2$	$0.1201^{+0.0010}_{-0.0011}$	$0.1207^{+0.0018}_{-0.0020}$	0.1199 ± 0.0009	0.1199 ± 0.0008
$100\theta_{\text{MC}}$	1.04073 ± 0.00048	1.04070 ± 0.00028	1.04075 ± 0.00013	1.04076 ± 0.00010
τ	0.055 ± 0.002	0.057 ± 0.009	0.057 ± 0.008	$0.055^{+0.002}_{-0.003}$
H_0	$66.64^{+1.71}_{-1.72}$	$66.76^{+1.82}_{-1.83}$	$66.74^{+1.74}_{-1.72}$	$66.79^{+1.69}_{-1.71}$
Ω_K	0.000 ± 0.002	$0.001^{+0.002}_{-0.003}$	0.000 ± 0.001	0.000 ± 0.001
$\log(10^{10} A_s)$	3.095 ± 0.004	3.100 ± 0.018	3.098 ± 0.017	3.095 ± 0.005
n_s	0.9638 ± 0.0042	$0.9625^{+0.0059}_{-0.0058}$	0.9643 ± 0.0026	0.9643 ± 0.0022
w_0	$-0.912^{+0.159}_{-0.195}$	$-0.918^{+0.172}_{-0.204}$	$-0.926^{+0.163}_{-0.190}$	$-0.938^{+0.142}_{-0.182}$
w_a	$-0.323^{+0.619}_{-0.444}$	$-0.330^{+0.643}_{-0.497}$	$-0.271^{+0.588}_{-0.460}$	$-0.213^{+0.548}_{-0.375}$
m_ν	$< 0.205 \text{ eV}$	$< 0.284 \text{ eV}$	$< 0.211 \text{ eV}$	$< 0.148 \text{ eV}$

Table X. Forecasted constraints at 68% C.L. (upper limits at 95% C.L.) from CMB+DESI+GWSS67 data for the experimental configurations in Table I in case of the Λ CDM+ Ω_k + Σm_ν + w + w_a extended model. Note the significant improvement in accuracy on H_0 and on the dark energy parameters w_0 and w_a with respect to the CMB+DESI case.

C. Figure of Merit

It is interesting to quantify the improvement of a GWSS prior by comparing the overall Figure of Merit for the cases considered. Given an experimental configuration and a set of N parameters p_i with $i = (1, \dots, N)$, we can define the FoM from the covariance matrix of uncertainties on p_i as (see e.g. [62, 97]):

$$\text{FoM} = (\det[\text{cov } p_i])^{-1/2} \quad (8)$$

that is proportional to the inverse of the volume of the constrained parameters space. It is important to stress that this FoM considers the whole parameter space and not just the dark energy parameters as in [72].

In Table XI we report the FoM for the two theoretical scenarios considered in this paper and for different combinations of datasets. The FoM are normalized to the S3deep, CMB only, value. As we can see, in the case of $\Lambda\text{CDM} + \Omega_k + \Sigma m_\nu + N_{\text{eff}} + w$ there is a significant improvement in FoM when the GWSS67 prior is included with the CMB data. The improvement is significant (between a factor ~ 50 and ~ 400) and larger in the case of the CMB-S4 dataset. A smaller but still significant improvement is present when the PGWSS67 prior is considered. This clearly shows that, once the geometrical degeneracies are broken by the introduction of the GWSS prior, there is a significantly improved parameter determination with this dataset. It is interesting also to note that the S3wide configuration has a constraining power that is superior to LiteBIRD+GWSS67 and S3deep+GWSS67. When the DESI dataset is included there is an improvement by a factor ~ 1000 and ~ 2400 . In this case the CMB dataset that would better benefit by the inclusion of the DESI data is S3deep. Both S3deep+DESI and LiteBIRD+DESI have a smaller FoM than S3wide+GWSS67, and S3wide+DESI has less constraining power than CMB-S4+GWSS67. When further including the GWSS67 prior the improvement in FoM is about a factor 2–3 with respect to the CMB+DESI case, clearly showing that GWSS will be useful in further constraining the parameter space. However, when considering the more pessimistic PGWSS67 prior the improvement with respect to the CMB+DESI case is just $\sim 10 - 20\%$.

In the case of the $\Lambda\text{CDM} + \Omega_k + \Sigma m_\nu + w_0 + w_a$ model the improvement in the FoM obtained by the inclusion of the GWSS67 prior in the case of the CMB data is about a factor of ~ 50 . With the DESI dataset the improvement is a factor of $\sim 1000 - 2400$. As we can see these improvements are smaller if compared to the $\Lambda\text{CDM} + \Omega_k + \Sigma m_\nu + N_{\text{eff}} + w$ scenario, showing that in this case the parameter degeneracies are more severe. When the GWSS67 prior is included the improvement is about a factor $\sim 4 - 6$, larger if compared with the similar data combination for the $\Lambda\text{CDM} + \Omega_k + \Sigma m_\nu + N_{\text{eff}} + w$ scenario. The combination of LiteBIRD, S3deep, and S3wide with DESI data has less constraining power than

CMB-S4+GWSS67. The inclusion of a PGWSS67 prior can improve by a $\sim 60\%$ the FoM of CMB-S4 and CMB-S4+DESI.

Finally, in order to better visualize the impact of a future prior on H_0 , we plot in Figure 7 the values of the FoM in function of 4 different expected accuracies on the Hubble constant: 4%, 3%, 2%, and 1%. We can firstly clearly see that the FoM will be in general larger in case of the " $w_0 + w_a$ " scenario with respect to the " $w_0 + N_{\text{eff}}$ " for any experimental configuration (with the exception of LiteBIRD). The inclusion of an external prior on the Hubble parameter is therefore more efficient in improving the constraints in the case of a " $w_0 + w_a$ " model, where dynamical dark energy is considered. Secondly, while in the CMB only scenario an improvement in the accuracy of H_0 is always reflected in a substantial increase in the FoM, it seems that in the case of CMB+DESI and for the " $w_0 + N_{\text{eff}}$ " model (the red lines in the figure) a significant increase is expected when moving to an accuracy below 2%. An improved accuracy in H_0 from 4% to 2% produces larger improvements in the FoM for the CMB+DESI dataset in the case of the " $w_0 + w_a$ " scenario.

IV. CONCLUSIONS

The recent observations of gravitational waves and electromagnetic emission produced by the merger of the binary neutron-star system GW170817 has introduced a complementary and direct method for measuring the Hubble constant. In the coming decade GW standard sirens are expected to produce constraints on H_0 with $\sim 1\%$ accuracy. At the same time, improved constraints are expected from CMB experiments and from BAO surveys. In an extended ΛCDM parameter space, where we have considered variations in curvature, neutrino mass, and the dark energy equation of state, we have found that a combination of future CMB and BAO data can constrain the Hubble constant at the level of 1.5–2%. A similar accuracy may be reached by the HLV network in the second year of observations if the the BNS rate is $R \geq 2800 \text{ Gpc}^{-3}\text{yr}^{-1}$, in agreement with current limits on R , or by the HLVI network after one year of observations with a more conservative BNS detection rate of $R \geq 1540 \text{ Gpc}^{-3}\text{yr}^{-1}$.

Gravitational wave standard sirens may reach a 1% measurement of H_0 within the decade, which when combined with future CMB data would constrain curvature to 0.3% and the dark energy equation of state to $\sim 5\%$. A GWSS measurement of the Hubble constant would also improve the constraints on these geometrical parameters coming from future CMB+BAO data by 30–40%. In addition, the current 2σ Hubble tension between CMB+BAO and supernova data could be strengthened to 5σ with the inclusion of standard siren constraints.

When we further include time variations in the dark energy equation of state, parameterizing its evolution with

Model	Dataset	LiteBIRD	S3deep	S3wide	CMB-S4
$\Lambda\text{CDM}+\Omega_k+\Sigma m_\nu+N_{\text{eff}}+w$	CMB	5	1	398	29236
	CMB+PGWSS67	110	40	12732	2.2×10^6
	CMB+GWSS67	262	104	50929	1.2×10^7
	CMB+DESI	6659	2415	383240	3.74×10^7
	CMB+DESI+PGWSS67	7735	2807	422008	4.06×10^7
	CMB+DESI+GWSS67	16928	5484	752879	7.39×10^7
$\Lambda\text{CDM}+\Omega_k+\Sigma m_\nu+w_0+w_a$	CMB	7	1	170	9223
	CMB+PGWSS67	111	18	2732	14402
	CMB+GWSS67	291	43	9231	589791
	CMB+DESI	13335	2394	227590	1.04×10^7
	CMB+DESI+PGWSS67	19458	3577	323789	1.6×10^7
	CMB+DESI+GWSS67	57928	11735	1.01×10^6	5.7×10^7

Table XI. Improvement with respect to simulated CMB data of the global Figure of Merit for the two theoretical scenarios considered in the paper and for different combination of datasets. The FoM is normalized to the S3deep CMB alone case that provides the less constraining results.

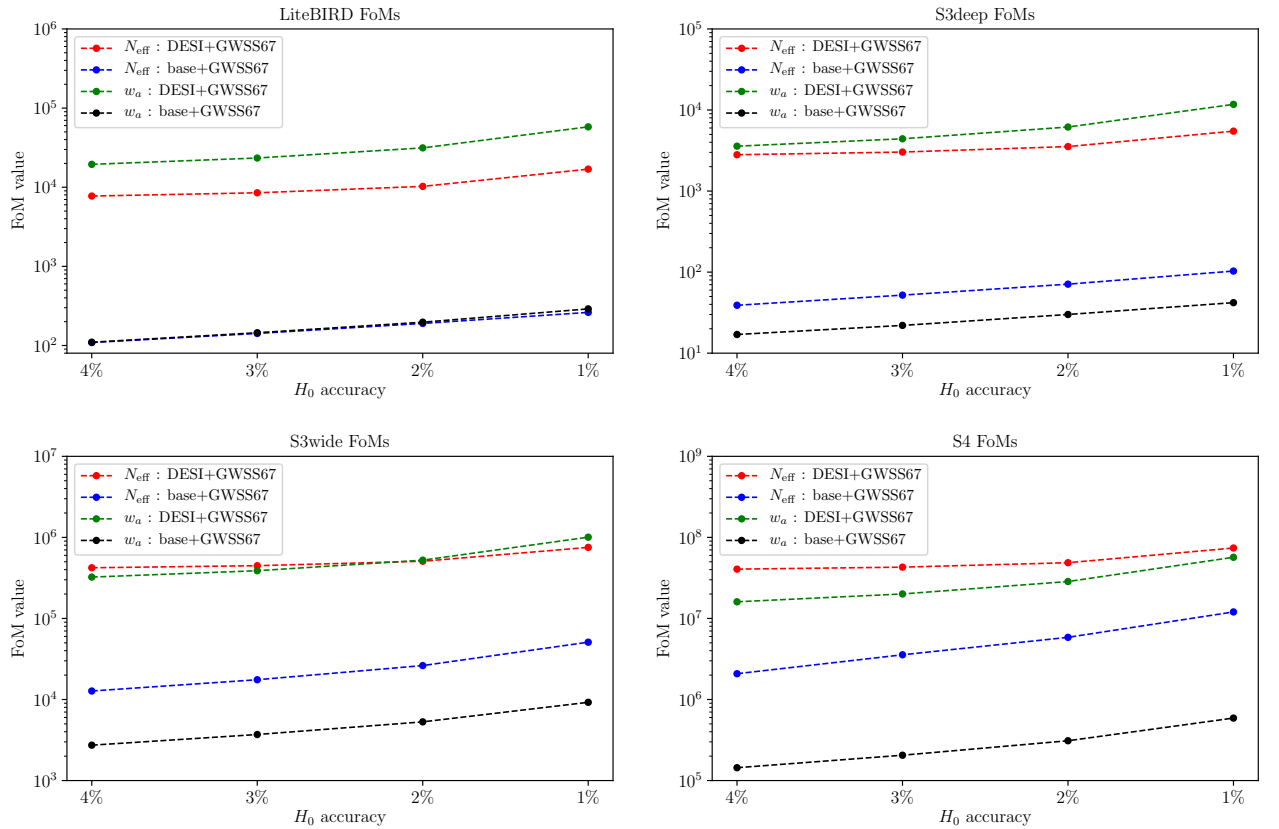


Figure 7. Figures of Merit for the theoretical models and experimental configurations considered in function of different priors on the Hubble parameter with a 4%, 3%, 2%, and 1% accuracy respectively. The assumed CMB datasets are LiteBIRD (Top Left), S3deep (Top Right), S3wide (Bottom Left), and CMB-S4 (Bottom Right).

a CPL function, we find that future CMB+BAO data will constrain the Hubble constant to $\sim 3\%$. This level of accuracy on H_0 can be independently reached by the HLV network of interferometers after the second year of operation if the BNS detection rate is $R > 3500 \text{ Gpc}^{-3}\text{yr}^{-1}$, a value again well inside current limits, or by the HLVJI network after one year of observations even considering a low BNS detection rate of $R = 320 \text{ Gpc}^{-3}\text{yr}^{-1}$. This standard siren measurement would therefore improve the CMB+BAO constraints on this model at the level of 10 – 30%.

Assuming a future H_0 accuracy of $\sim 1\%$ from standard sirens, as to be expected within the decade, we find that the constraints on the dark energy equation of state parameters w_0 and w_a from future CMB+BAO datasets can be improved by a factor 1.6–2.8. We conclude that standard siren measurements by the HLV and HLVJI gravitational-wave detector networks over the coming decade may significantly improve our understanding of cosmology.

We have also found that even a more pessimistic determination of H_0 , with a $\sim 4\%$ accuracy can significantly improve the constraints from CMB alone data in case of a $\Lambda\text{CDM} + \Omega_k + \Sigma m_\nu + N_{\text{eff}} + w$ model and from CMB alone and CMB+DESI data in case of a $\Lambda\text{CDM} + \Omega_k + \Sigma m_\nu + w_0 + w_a$ model.

Finally it is clearly worth mentioning that similar constraints on H_0 and dark energy parameters could come by combining CMB and BAO data with other complementary probes such as supernovae and cosmic shear (see e.g. [54, 98]). In this case future constraints from GWSS will play a crucial role in confirming these results and cross-validating the different approaches. In addition, these comparisons offer the exciting possibility of discovering new physics beyond the Λ -CDM scenario.

ACKNOWLEDGMENTS

EDV acknowledges support from the European Research Council in the form of a Consolidator Grant with number 681431. AM thanks the University of Manchester and the Jodrell Bank Center for Astrophysics for hospitality. AM and FR are supported by TASP, iniziativa specifica INFN. DEH was partially supported by NSF grant PHY-1708081. He was also supported by the Kavli Institute for Cosmological Physics at the University of Chicago through NSF grant PHY-1125897 and an endowment from the Kavli Foundation. DEH also gratefully acknowledges support from the Marion and Stuart Rice Award. We thank Cristiano Palomba for useful comments.

-
- [1] B. F. Schutz, *Nature* **323** (1986) 310. doi:10.1038/323310a0
 - [2] Holz, D. E. & Hughes, S. A. 2005, *Astrophys. J.*, 629, 15.
 - [3] S. Nissanke, D. E. Holz, N. Dalal, S. A. Hughes, J. L. Sievers and C. M. Hirata, [arXiv:1307.2638](#) [astro-ph.CO].
 - [4] N. Dalal, D. E. Holz, S. A. Hughes and B. Jain, *Phys. Rev. D* **74** (2006) 063006 doi:10.1103/PhysRevD.74.063006 [[astro-ph/0601275](#)].
 - [5] H. Y. Chen, M. Fishbach and D. E. Holz, [arXiv:1712.06531](#) [astro-ph.CO].
 - [6] A. Nishizawa, *Phys. Rev. D* **96** (2017) no.10, 101303 doi:10.1103/PhysRevD.96.101303 [[arXiv:1612.06060](#) [astro-ph.CO]].
 - [7] N. Seto and K. Kyutoku, *Mon. Not. Roy. Astron. Soc.* **475** (2018) no.3, 4133 doi:10.1093/mnras/sty090 [[arXiv:1710.06424](#) [astro-ph.CO]].
 - [8] R. Nair, S. Bose and T. D. Saini, *Phys. Rev. D* **98** (2018) no.2, 023502 doi:10.1103/PhysRevD.98.023502 [[arXiv:1804.06085](#) [astro-ph.CO]].
 - [9] S. Vitale and H. Y. Chen, *Phys. Rev. Lett.* **121** (2018) no.2, 021303 doi:10.1103/PhysRevLett.121.021303 [[arXiv:1804.07337](#) [astro-ph.CO]].
 - [10] [The LIGO Scientific and The Virgo Collaborations], doi:10.1103/PhysRevLett.119.161101 [[arXiv:1710.05832](#) [gr-qc]].
 - [11] Abbott, B. P., Abbott, R., Abbott, T. D., et al. 2017, *Astrophys. J.*, 848, L12.
 - [12] Coulter, D. A., Foley, R. J., Kilpatrick, C. D., et al. 2017, *Science*, 358, 1556.
 - [13] Soares-Santos, M., Holz, D. E., Annis, J., et al. 2017, *Astrophys. J.*, 848, L16.
 - [14] B. P. Abbott *et al.* [The LIGO Scientific and The Virgo and The 1M2H and The Dark Energy Camera GW-EM and the DES and The DLT40 and The Las Cumbres Observatory and The VINROUGE and The MASTER Collaborations], doi:10.1038/nature24471 [arXiv:1710.05835](#) [astro-ph.CO].
 - [15] A. G. Riess *et al.*, [arXiv:1604.01424](#) [astro-ph.CO].
 - [16] A. G. Riess *et al.*, [arXiv:1804.10655](#) [astro-ph.CO].
 - [17] N. Aghanim *et al.* [Planck Collaboration], [arXiv:1807.06209](#) [astro-ph.CO].
 - [18] N. Aghanim *et al.* [Planck Collaboration], *Astron. Astrophys.* **596** (2016) A107 doi:10.1051/0004-6361/201628890 [[arXiv:1605.02985](#) [astro-ph.CO]].
 - [19] W. L. Freedman, *Nat. Astron.* **1** (2017) 0169 [[arXiv:1706.02739](#) [astro-ph.CO]].
 - [20] P. A. R. Ade *et al.* [Planck Collaboration], [arXiv:1502.01589](#) [astro-ph.CO].
 - [21] E. Di Valentino, A. Melchiorri and J. Silk, *Phys. Lett. B* **761** (2016) 242 doi:10.1016/j.physletb.2016.08.043 [[arXiv:1606.00634](#) [astro-ph.CO]].
 - [22] E. Di Valentino, A. Melchiorri, E.V. Linder, J. Silk, *Phys. Rev. D* **96**, 023523 (2017) [[arXiv:1704.00762](#)].
 - [23] E. Di Valentino, E. Linder and A. Melchiorri, [arXiv:1710.02153](#) [astro-ph.CO].
 - [24] M. M. Zhao, D. Z. He, J. F. Zhang and X. Zhang, [arXiv:1703.08456](#) [astro-ph.CO].
 - [25] W. Yang, R. C. Nunes, S. Pan and D. F. Mota, [arXiv:1703.02556](#) [astro-ph.CO].
 - [26] V. Prilepina and Y. Tsai, [arXiv:1611.05879](#) [hep-ph].

- [27] B. Santos, A. A. Coley, N. C. Devi and J. S. Alcaniz, JCAP **1702** (2017) no.02, 047 doi:10.1088/1475-7516/2017/02/047 [[arXiv:1611.01885](#) [astro-ph.CO]].
- [28] S. Kumar and R. C. Nunes, Phys. Rev. D **94** (2016) no.12, 123511 doi:10.1103/PhysRevD.94.123511 [[arXiv:1608.02454](#) [astro-ph.CO]].
- [29] T. Karwal and M. Kamionkowski, Phys. Rev. D **94**, no. 10, 103523 (2016) doi:10.1103/PhysRevD.94.103523 [[arXiv:1608.01309](#) [astro-ph.CO]].
- [30] M. Benetti, L. L. Graef and J. S. Alcaniz, [[arXiv:1712.00677](#) [astro-ph.CO]].
- [31] P. Ko and Y. Tang, Phys. Lett. B **762** (2016) 462 doi:10.1016/j.physletb.2016.10.001 [[arXiv:1608.01083](#) [hep-ph]].
- [32] M. Archidiacono, S. Gariazzo, C. Giunti, S. Hannestad, R. Hansen, M. Laveder and T. Tram, JCAP **1608**, no. 08, 067 (2016) doi:10.1088/1475-7516/2016/08/067 [[arXiv:1606.07673](#) [astro-ph.CO]].
- [33] Q. G. Huang and K. Wang, Eur. Phys. J. C **76** (2016) no.9, 506 doi:10.1140/epjc/s10052-016-4352-x [[arXiv:1606.05965](#) [astro-ph.CO]].
- [34] Y. Zhang, H. Zhang, D. Wang, Y. Qi, Y. Wang and G. B. Zhao, [[arXiv:1703.08293](#) [astro-ph.CO]].
- [35] G. B. Zhao *et al.*, [[arXiv:1701.08165](#) [astro-ph.CO]].
- [36] J. Sola, J. d. C. Perez and A. Gomez-Valent, [[arXiv:1703.08218](#) [astro-ph.CO]].
- [37] C. Brust, Y. Cui and K. Sigurdson, [[arXiv:1703.10732](#) [astro-ph.CO]].
- [38] E. Di Valentino, A. Melchiorri and O. Mena, Phys. Rev. D **96** (2017) no.4, 043503 doi:10.1103/PhysRevD.96.043503 [[arXiv:1704.08342](#) [astro-ph.CO]].
- [39] E. Di Valentino, C. Bøehm, E. Hivon and F. R. Bouchet, Phys. Rev. D **97** (2018) no.4, 043513 doi:10.1103/PhysRevD.97.043513 [[arXiv:1710.02559](#) [astro-ph.CO]].
- [40] W. Yang, S. Pan, E. Di Valentino, R. C. Nunes, S. Vagnozzi and D. F. Mota, [[arXiv:1805.08252](#) [astro-ph.CO]].
- [41] E. Di Valentino, A. Melchiorri and J. Silk, Phys. Rev. D **92** (2015) no.12, 121302 doi:10.1103/PhysRevD.92.121302 [[arXiv:1507.06646](#) [astro-ph.CO]].
- [42] G. B. Zhao *et al.*, Nat. Astron. **1**, no. 9, 627 (2017) doi:10.1038/s41550-017-0216-z [[arXiv:1701.08165](#) [astro-ph.CO]].
- [43] E. Di Valentino, Nat. Astron. **1**, no. 9, 569 (2017) doi:10.1038/s41550-017-0236-8 [[arXiv:1709.04046](#) [physics.pop-ph]].
- [44] Hu, W. 2005, Observing Dark Energy, 215.
- [45] C. L. MacLeod and C. J. Hogan, Phys. Rev. D **77** (2008) 043512 doi:10.1103/PhysRevD.77.043512 [[arXiv:0712.0618](#) [astro-ph]].
- [46] C. Cutler and D. E. Holz, Phys. Rev. D **80** (2009) 104009 doi:10.1103/PhysRevD.80.104009 [[arXiv:0906.3752](#) [astro-ph.CO]].
- [47] B. S. Sathyaprakash, B. F. Schutz and C. Van Den Broeck, Class. Quant. Grav. **27** (2010) 215006 doi:10.1088/0264-9381/27/21/215006 [[arXiv:0906.4151](#) [astro-ph.CO]].
- [48] W. Zhao, C. Van Den Broeck, D. Baskaran and T. G. F. Li, Phys. Rev. D **83** (2011) 023005 doi:10.1103/PhysRevD.83.023005 [[arXiv:1009.0206](#) [astro-ph.CO]].
- [49] W. Del Pozzo, Phys. Rev. D **86** (2012) 043011 doi:10.1103/PhysRevD.86.043011 [[arXiv:1108.1317](#) [astro-ph.CO]].
- [50] A. Nishizawa, K. Yagi, A. Taruya and T. Tanaka, Phys. Rev. D **85** (2012) 044047 doi:10.1103/PhysRevD.85.044047 [[arXiv:1110.2865](#) [astro-ph.CO]].
- [51] S. R. Taylor and J. R. Gair, Phys. Rev. D **86** (2012) 023502 doi:10.1103/PhysRevD.86.023502 [[arXiv:1204.6739](#) [astro-ph.CO]].
- [52] N. Tamanini, C. Caprini, E. Barausse, A. Sesana, A. Klein and A. Petiteau, JCAP **1604** (2016) no.04, 002 doi:10.1088/1475-7516/2016/04/002 [[arXiv:1601.07112](#) [astro-ph.CO]].
- [53] E. Belgacem, Y. Dirian, S. Foffa and M. Maggiore, [[arXiv:1805.08731](#) [gr-qc]].
- [54] S. M. Feeney, H. V. Peiris, A. R. Williamson, S. M. Nisanke, D. J. Mortlock, J. Alsing and D. Scolnic, [[arXiv:1802.03404](#) [astro-ph.CO]].
- [55] H. Audley *et al.*, (2017), [[arXiv:1702.00786](#) [astro-ph.IM]].
- [56] B. Sathyaprakash *et al.*, Class. Quant. Grav., 29, 124013 (2012), [Erratum: Class. Quant. Grav.30,079501(2013)], [[arXiv:1206.0331](#) [gr-qc]].
- [57] B. P. Abbott *et al.* [LIGO Scientific Collaboration], Class. Quant. Grav. **34** (2017) no.4, 044001 doi:10.1088/1361-6382/aa51f4 [[arXiv:1607.08697](#) [astro-ph.IM]].
- [58] Abbott, B. P., Abbott, R., Abbott, T. D., *et al.* 2018, Living Reviews in Relativity, 21, 3.
- [59] T. Matsumura, Y. Akiba, J. Borrill, Y. Chinone, M. Dobbs, H. Fuke, A. Ghribi, M. Hasegawa, K. Hattori, M. Hattori, *et al.*, Journal of Low Temperature Physics 176, 733 (2014), 1311.2847; A. Suzuki *et al.*, [[arXiv:1801.06987](#) [astro-ph.IM]].
- [60] K. N. Abazajian *et al.* [CMB-S4 Collaboration], [[arXiv:1610.02743](#) [astro-ph.CO]].
- [61] M. Levi *et al.* [DESI Collaboration], [[arXiv:1308.0847](#) [astro-ph.CO]].
- [62] E. Di Valentino *et al.* [CORE Collaboration], [[arXiv:1612.00021](#) [astro-ph.CO]].
- [63] B. P. Abbott *et al.*, Physical Review D, Volume 95, Issue 6, id.062003.
- [64] B. P. Abbott *et al.*, Physical Review Letters, Volume 118, Issue 22, id.221101
- [65] Karki, S., Tuyenbayev, D., Kandhasamy, S., *et al.* 2016, Review of Scientific Instruments, 87, 114503.
- [66] Huterer, D. & Shafer, D. L. 2018, Reports on Progress in Physics, 81, 16901.
- [67] R. Laureijs *et al.* [EUCLID Collaboration], [[arXiv:1110.3193](#) [astro-ph.CO]].
- [68] R. Mandelbaum *et al.*, Astrophys. J. Suppl. 212 (2014) 5, [[arXiv:1308.4982](#)].
- [69] Z.-M. Ma, W. Hu, and D. Huterer, Astrophys. J. 636 (2005) 21–29, [[astro-ph/0506614](#)].
- [70] Riess, A. G., Macri, L. M., Hoffmann, S. L., *et al.* 2016, Astrophys. J., 826, 56.
- [71] Uddin, S. A., Mould, J., Lidman, C., *et al.* 2017, Astrophys. J., 848, 56.
- [72] D. Weinberg *et al.*, Physics Reports, Volume 530, Issue 2, p. 87-255.
- [73] E. Di Valentino and A. Melchiorri, Phys. Rev. D **97**, no. 4, 041301 (2018) doi:10.1103/PhysRevD.97.041301 [[arXiv:1710.06370](#) [astro-ph.CO]].
- [74] A. D. Linde, JCAP **0305** (2003) 002 doi:10.1088/1475-7516/2003/05/002 [[astro-ph/0303245](#)].

- [75] F. Capozzi, E. Di Valentino, E. Lisi, A. Marrone, A. Melchiorri and A. Palazzo, Phys. Rev. D **95** (2017) no.9, 096014 doi:10.1103/PhysRevD.95.096014 [[arXiv:1703.04471](#) [hep-ph]].
- [76] D. Baumann, D. Green and B. Wallisch, Phys. Rev. Lett. **117** (2016) no.17, 171301 doi:10.1103/PhysRevLett.117.171301 [[arXiv:1604.08614](#) [astro-ph.CO]].
- [77] P. F. de Salas, M. Lattanzi, G. Mangano, G. Miele, S. Pastor and O. Pisanti, Phys. Rev. D **92** (2015) no.12, 123534 doi:10.1103/PhysRevD.92.123534 [[arXiv:1511.00672](#) [astro-ph.CO]].
- [78] M. Chevallier and D. Polarski, Int. J. Mod. Phys. D **10**, 213 (2001).
- [79] E.V. Linder, Phys. Rev. Lett. **90**, 091301 (2003).
- [80] W. Hu, Phys. Rev. D **71** (2005) 047301 doi:10.1103/PhysRevD.71.047301 [[astro-ph/0410680](#)].
- [81] A. Lewis, A. Challinor and A. Lasenby, Astrophys. J. **538** (2000) 473 doi:10.1086/309179 [[astro-ph/9911177](#)].
- [82] A. Lewis and S. Bridle, Phys. Rev. D **66**, 103511 (2002) [[astro-ph/0205436](#)].
- [83] L. Capparelli, E. Di Valentino, A. Melchiorri and J. Chluba, [arXiv:1712.06965](#) [astro-ph.CO].
- [84] F. Renzi, E. Di Valentino and A. Melchiorri, [arXiv:1712.08758](#) [astro-ph.CO].
- [85] L. Perotto, J. Lesgourgues, S. Hannestad, H. Tu and Y. Y. Y. Wong, JCAP **0610** (2006) 013 doi:10.1088/1475-7516/2006/10/013 [[astro-ph/0606227](#)].
- [86] R. Allison, P. Caucal, E. Calabrese, J. Dunkley and T. Louis, Phys. Rev. D **92** (2015) no.12, 123535 doi:10.1103/PhysRevD.92.123535 [[arXiv:1509.07471](#) [astro-ph.CO]].
- [87] A. Font-Ribera, P. McDonald, N. Mostek, B. A. Reid, H. J. Seo and A. Slosar, JCAP **1405**, 023 (2014) doi:10.1088/1475-7516/2014/05/023 [[arXiv:1308.4164](#) [astro-ph.CO]].
- [88] G. E. Addison, D. J. Watts, C. L. Bennett, M. Halpern, G. Hinshaw and J. L. Weiland, Astrophys. J. **853** (2018) no.2, 119 doi:10.3847/1538-4357/aaa1ed [[arXiv:1707.06547](#) [astro-ph.CO]].
- [89] S. Sato *et al.*, J. Phys. Conf. Ser. **840** (2017) no.1, 012010. doi:10.1088/1742-6596/840/1/012010
- [90] Fishbach, M., Holz, D. E. & Farr, W. M. 2018, ArXiv e-prints, [arXiv:1805.10270](#).
- [91] B. P. Abbott *et al.* [LIGO Scientific Collaboration and Virgo Collaboration], Phys. Rev. Lett. **119**, 161101, 2017.
- [92] N. Gupte and I. Bartos, [arXiv:1808.06238](#) [astro-ph.HE].
- [93] D. Scolnic *et al.*, The Astrophysical Journal Letters, Volume 852, Issue 1, article id. L3, 7 pp. (2018).
- [94] Bond, J., Efstathiou, G., & Tegmark, M., Forecasting cosmic parameter errors from microwave background anisotropy experiments. 1997, MNRAS, **291**, L33, [arXiv:astro-ph/9702100](#).
- [95] Zaldarriaga, M., Spergel, D. N., & Seljak, U., Microwave background constraints on cosmological parameters. 1997, ApJ, **488**, 1, [arXiv:astro-ph/9702157](#).
- [96] A. Melchiorri and L. M. Griffiths, New Astron. Rev. **45** (2001) 321 doi:10.1016/S1387-6473(00)00154-8 [[astro-ph/0011147](#)].
- [97] C. Bennett *et al.*, The Astrophysical Journal Supplement, Volume 208, Issue 2, article id. 20, 54 pp. (2013).
- [98] É. Aubourg *et al.*, Phys. Rev. D **92** (2015) no.12, 123516 doi:10.1103/PhysRevD.92.123516 [[arXiv:1411.1074](#) [astro-ph.CO]].